High-energy mode-locked fiber lasers using multiple transmission filters and a genetic algorithm

Xing Fu and J. Nathan Kutz*

Department of Applied Mathematics, University of Washington, Seattle, WA 98195-2420 USA

*kutz@amath.washington.edu

Abstract: We theoretically demonstrate that in a laser cavity mode-locked by nonlinear polarization rotation (NPR) using sets of waveplates and passive polarizer, the energy performance can be significantly increased by incorporating multiple NPR filters. The NPR filters are engineered so as to mitigate the multi-pulsing instability in the laser cavity which is responsible for limiting the single pulse per round trip energy in a myriad of mode-locked cavities. Engineering of the NPR filters for performance is accomplished by implementing a genetic algorithm that is capable of systematically identifying viable and optimal NPR settings in a vast parameter space. Our study shows that five NPR filters can increase the cavity energy by approximately a factor of five, with additional NPRs contributing little or no enhancements beyond this. With the advent and demonstration of electronic controls for waveplates and polarizers, the analysis suggests a general design and engineering principle that can potentially close the order of magnitude energy gap between fiber based mode-locked lasers and their solid state counterparts.

OCIS codes: (140.4050) Mode-locked lasers; (320.7090) Ultrafast lasers.

References and links

1. D. J. Richardson, J. Nilsson, and W. A. Clarkson, "High power fiber lasers: current status and future perspectives," J. Opt. Soc. Am. B **27**, B63-B92 (2010).
2. H. A. Haus, "Mode-locking of lasers," IEEE J. Sel. Top. Quant. Elec. **6**, 1173-1185 (2000).
3. K. Tamura, E.P. Ippen, H.A. Haus, and L.E. Nelson, "77-fs Pulse generation from a stretched-pulse mode-locked all-fiber ring laser," Opt. Lett. **18**, 1080-1082 (1993).
4. K. Tamura and M. Nakazawa, "Optimizing power extraction in stretched pulse fiber ring lasers," App. Phys. Lett. **67**, 3691-3693 (1995).
5. G. Lenz, K. Tamura, H. A. Haus, and E. P. Ippen, "All-solid-state femtosecond source at 1.55 μm," Opt. Lett. **20**, 1289-1291 (1995).
6. F. Ö. Ilday, J. Buckley, and F. W. Wise, "Self-similar evolution of parabolic pulses in a laser cavity," Phys. Rev. Lett. **92**, 213902 (2004).
7. W. H. Renninger, A. Chong, and F. W. Wise. "Self-similar pulse evolution in an all-normal-dispersion laser." Phys. Rev. A **82**, 021805 (2010).
8. B. Bale and S. Wabnitz, "Strong spectral filtering for a mode-locked similariton fiber laser," Opt. Lett. **35**, 2466-2468 (2010).
9. A. Chong, W. H. Renninger, and F. W. Wise, "Properties of normal-dispersion femtosecond fiber lasers," J. Opt. Soc. Am. B **25**, 140-148 (2008).
10. S. Namiki, E. P. Ippen, H. A. Haus, and C. X. Yu, "Energy rate equations for mode-locked lasers," J. Opt. Soc. Am. B **14**, 2099-2111 (1997).

#179642 - $15.00 USD Received 12 Nov 2012; revised 13 Feb 2013; accepted 3 Mar 2013; published 8 Mar 2013

11. B. G. Bale, K. Kieu, J. N. Kutz, and F. Wise, "Transition dynamics for multi-pulsing in mode-locked lasers," Opt. Express **17**, 23137-23146 (2009).
12. E. Ding, E. Shlizerman, and J. N. Kutz, "Generalized master equation for high-energy passive mode-locking: the sinusoidal Ginzburg-Landau equation," IEEE J. Quant. Electron. **47**, 705-714 (2011).
13. F. Li, P. K. A. Wai, and J. N. Kutz, "Geometrical description of the onset of multi-pulsing in mode-locked laser cavities," J. Opt. Soc. Am. B **27**, 2068-2077 (2010).
14. R. Herda, O. G. Okhotnikov, E. U. Rafailov, W. Sibbett, P. Crittenden, and A. Starodumov, "Semiconductor quantum-dot saturable absorber mode-locked fiber laser," IEEE Photon. Technol. Lett. **18**, 157-159 (2006).
15. S. Y. Set, H. Yaguchi, Y. Tanaka, and M. Jablonski, "Laser mode locking using a saturable absorber incorporating carbon nanotubes," J. Lightwave Technol. **22**, 51-56 (2004).
16. S. Yamashita, Y. Inoue, S. Maruyama, Y. Murakami, H. Yaguchi, M. Jablonski, and S. Y. Set, "Saturable absorbers incorporating carbon nanotubes directly synthesized onto substrates and fibersand their application to mode-locked fiber lasers," Opt. Lett. **29**, 1581-1583 (2004).
17. Z. Sun, T. Hasan, F. Torrisi, D. Popa, G. Privitera, F. Wang, F. Bonaccorso, D. M. Basko, and A. C. Ferrari, "Graphene mode-locked ultrafast laser," ACS Nano **4**, 803-810 (2010).
18. H. Zhang, "Large energy soliton erbium-doped fiber laser with a graphene-polymer composite mode locker," App. Phys. Lett. **95**, 141103 (2009).
19. H. Zhang, D. Y. Tang, L. M. Zhao, Q. L. Bao, and K. P. Loh, "Large energy mode locking of an erbium-doped fiber laser with atomic layer graphene," Opt. Express **17**, 17630-17635 (2009).
20. F. Li, E. Ding, J. N. Kutz, and P. K. A. Wai, "Dual transmission filters for enhanced energy in mode-locked fiber lasers," Opt. Express **19**, 23408-23419 (2011).
21. P. Grelu, W. Chang, A. Ankiewicz, J. M. Soto-Crespo, and N. Akhmediev, "Dissipative soliton resonance as a guideline for high-energy pulse laser oscillators," J. Opt. Soc. Am. B **27,** 2336-2341 (2010).
22. E. Ding, P. Grelu, and J. N. Kutz, "Dissipative soliton resonance in a passively mode-locked fiber laser," Opt. Lett. **36**, 1146-1148 (2011).
23. X. Shen, W. Li, M. Yan, and H. Zeng, "Electronic control of nonlinear-polarization-rotation mode locking in Yb-doped fiber lasers," Opt. Lett. **37**, 3426-3428 (2012).
24. E. Ding and J. N. Kutz, "Operating regimes and performance optimization in mode-locked fiber lasers," Optics and Spectroscopy **111**, 166-177 (2011).
25. C. R. Menyuk, "Pulse propagation in an elliptically birefringent Kerr media," IEEE J. Quant. Electron. **25**, 2674-2682 (1989).
26. C. R. Menyuk, "Nonlinear pulse propagation in birefringent optical fibers," IEEE J. Quant. Electron. **23**, 174-176 (1987).

1. Introduction

Despite more than two decades of development, mode-locked lasers have continued to make tremendous strides in engineering performance, both in terms of output energy and peak powers. Indeed, Richardson et al. [1] observed that in the past decade alone an average factor of 1.7 per year increase in power has been achieved, yielding approximately a two orders of magnitude power increase in the decade. Moreover, they note that this increase in performance is much more pronounced than increases in their solid-state counterparts. Such performance gains have raised hopes that fiber lasers, whose significant advantageous over solid-state designs are highlighted by Richardson et al. [1], may eventually provide a practical and low-cost engineering solution that competes directly with today's solid state lasers.

To be more directed in our mode-locking appraisal, the focus of this manuscript will be on one of the most commercially successful mode-locked lasers developed to date: a nonlinear polarization rotation (NPR) based passive fiber laser cavity that uses a combination of waveplates and a polarizer for achieving saturable absorption [2]. Laser cavities based upon this operating principle have evolved from delivering soliton-like mode-locking with pulse energies of approximately 0.1 nJ to delivering more exotic propagation behavior and mode-locking pulse shapes. In particular, dispersion-managed (stretched-pulse) soliton lasers deliver $\approx$1 nJ [3–5], similariton lasers peak around 10-20 nJ [6–8], and the ANDi laser design [9] is capable of achieving energies of approximately 40 nJ. Despite the tremendous performance increases, there is a ubiquitous and fundamental power/energy limitation that must be considered: the so-called multi-pulsing instability (MPI) [10–13]. MPI is the critical impediment for the design

#179642 - $15.00 USD Received 12 Nov 2012; revised 13 Feb 2013; accepted 3 Mar 2013; published 8 Mar 2013

and optimization of high-performance fiber lasers. Indeed, MPI imposes limitations on both NPR based lasers as well as those whose saturable absorption are generated from quantum dot doped fibers [14], carbon nanotubes [15, 16] and/or graphene [17–19].

Given its impact, methods for circumventing or suppressing MPI are highly desirable, especially as this is critical for achieving high energies. One method for doing so involves the so-called *dissipative soliton resonance* (DSR) in which a prescribed balance of physical effects are carefully enforced so as to allow for an indefinite increase in energy of a mode-locked pulse [21, 22]. Interestingly, as the DSR solutions increase in energy, their corresponding pulse widths increase likewise, thus no longer preserving the ultra-fast nature of the mode-locking configuration. Moreover, the peak pulse intensity does not scale with the increased energy. More recently, it was shown by Li et al. [20], based upon a geometrical viewpoint of the transmission curves [13], that adding one extra set of waveplates and polarizers generates a second nonlinear transmission function which allows for the suppression of the MPI effect. Specifically, it was demonstrated through numerical simulations that the cavity energy could be doubled in the dual-NPR configuration. In this manuscript, we develop further the idea of multiple transmission functions for enhancing performance. In particular, we demonstrate that adding multiple sets of waveplates and polarizers allows for significant suppression of the MPI effect, thus allowing for increase in the cavity energy by a factor of 5. For an ANDi laser [9], such an engineering solution would allow one to reach 200 nJ per pulse in energy from the fiber laser. However, engineering such performance is difficult to do in practice given the tuning required in the angles of the three waveplates and polarizer for generating the desired transmission curve for each NPR. Thus in addition to exploiting multiple transmission curves, we develop an optimization algorithm, based upon a genetic algorithm, that allows for effective exploration and evaluation of the high-dimensional parameter space. This allows for an efficient method for finding regions of peak performance and energy enhancement. Without such an algorithm, using many transmission curves generates an intractable engineering problem.

The manuscript is outlined as follows. In Sec. 2, the principle of operation is outlined with emphasis given to a geometrical interpretation of the effective transmission curve [13]. Section 3 introduces the NPR laser cavity equations which are governed by the coupled nonlinear Shrödinger equations (CNLS) with Jones matrices introduced to model the saturable absorption induced by the the NPR. In Sec. 4, a multi-grid genetic algorithm is developed in order to solve the parameter tuning problem introduced by the multiple NPRs. The numerical simulation results, which show significant energy enhancement, are shown in Sec. 5. The paper is concluded in Sec. 6 with a summary of the results and comments about the future outlook of such MPI suppression strategies.

2. Principle of operation

The key ideas for engineering the transmission curve for performance enhancement are developed by Li et al. [13, 20]. These ideas will be briefly revisited here in order to motivate the use of multiple transmission curves for significant energy gains in the cavity. To begin, it is well known that the standard combination of waveplates and polarizer in a mode-locked cavity produces a periodic transmission curve. In most theoretical models, most notably the commonly used master equation [2], the transmission curve is Taylor expanded about the first transmission peak, thus resulting in a cubic or cubic-quintic model for the saturable absorption of the waveplates and polarizer. Such theoretical treatments are thus incapable of modeling the multiple transmission peaks necessary for achieving the high energy mode-locking advocated here.

To be more precise, the geometrical description developed previously [13] shows that the multiple transmission windows can be exploited to stabilize and push mode-locked pulses to higher-energy states. Key to achieving this goal is the ability to engineer the transmission curve,

#179642 - $15.00 USD Received 12 Nov 2012; revised 13 Feb 2013; accepted 3 Mar 2013; published 8 Mar 2013

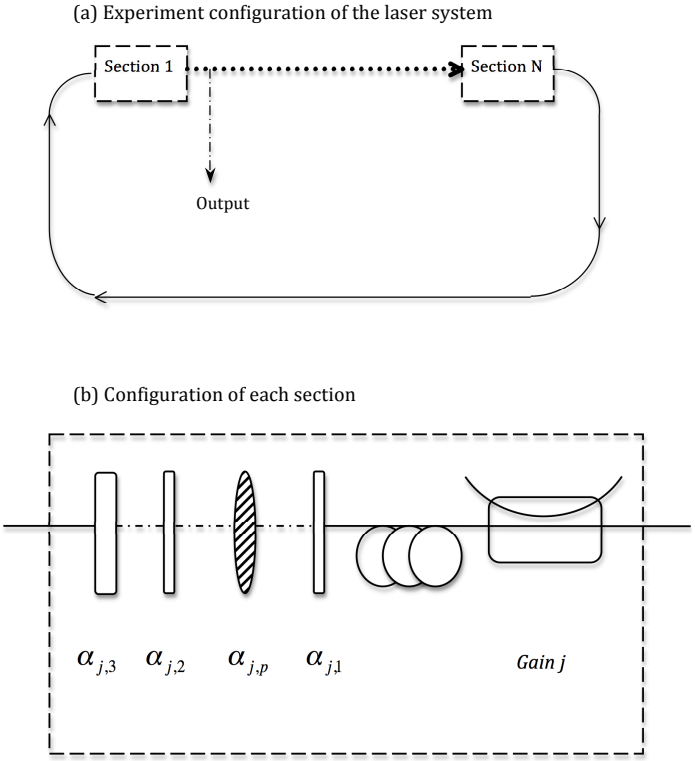

Fig. 1. (a) Experimental configuration of the multiple transmission filters ring cavity laser system that includes *N* NPR sections. The output of the lasers is taken between the 1st and 2nd NPR section. (b) Each NPR section contains two quarter-wave plates ($\alpha_{j,1}$ and $\alpha_{j,2}$), one half-wave plate ($\alpha_{j,3}$), one passive polarizer ($\alpha_{j,p}$), one amplifier and one gain source. Thus a minimum of 6 parameters must be tuned in each NPR section.

which can be done by adjusting the waveplate and polarizer angles. Indeed, the geometrical description showed that proper engineering of the transmission curve could allow mode-locking to naturally occur on the higher transmission windows instead of going through the MPI. These findings where recently confirmed by full component-by-component simulations of the laser cavity with two sets of waveplates/polarizer [20]. Indeed, by proper engineering, the cavity energy could be doubled with the inclusion of a second set of waveplates and polarizer.

To illustrate the concept in principle, consider the combination of transfer functions, denoted by T_j with $j = 1,2,...,N$, which are each produced by a particular setting of the waveplates and polarizer. Figure 1 demonstrates the physical setup that captures the fundamental principle expounded. In Fig. 1(a), a physically realizable cavity is shown with *N* sets of waveplates and polarizers. Each of these sets generates a nonlinear, periodic transmission T_1, T_2, ... , T_N respectively. A detail of each section of the fiber laser is shown in Fig. 1(b) where the waveplate and polarizer dynamics produces the transmission response T_j. In both Fig. 1(a) and 1(b), the gain elements are optional in the systems. It can be adopted to amplify the pulse after each

#179642 - $15.00 USD Received 12 Nov 2012; revised 13 Feb 2013; accepted 3 Mar 2013; published 8 Mar 2013

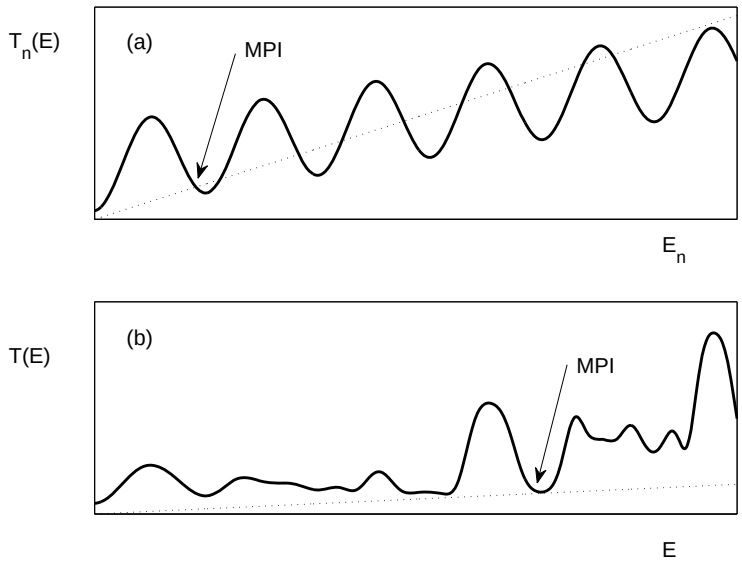

Fig. 2. (a) Prototypical example of the periodic transmission function $T_n(E)$ of a single NPR. As shown in Ref. [13,20], the onset of MPI occurs when the transmission curve intersects the small signal gain threshold (dotted line). Thus noise fluctuations below the dotted line would produce a new mode-locked pulse and induce MPI. (b) Prototypical example of the transmission function $T(E)$ given two periodic transmission filters used together as in (1). In this case, the onset of MPI is greatly suppressed and higher energy mode-locked states can be achieved [20]. Our goal is to engineer $T(E)$ using multiple transmission curves in order to achieve optimal mode-locking performance.

NPR if desired, giving more flexibility in the engineering design of the transmission function. As shown in Li et al. [20], additional gain elements are not necessary required for achieving higher-energy mode-locking.

As a concrete example, consider the case of two transmission curves (two waveplate and polarizers). The overall cavity transmission curve as a function of the electric field energy E is approximated by the combination

$$T(E) = T_2(T_1(E)E)T_1(E) \tag{1}$$

where $T(E)$ is the effective transmission curve generated from the successive application of T_1 and T_2. It is this flexibility that allows for the creation of the ideal transmission curves suggested for overcoming MPI [13]. Essentially, this allows for the generation of transmission functions T_1 and T_2 that have significantly different periodic openings in their transmission windows. Figure 2 demonstrates the basic principle by illustrating both a single periodic transmission function, T_n (with $n = 1,2$) along with the effective transmission function $T(E)$ given by (1). The dotted line is the instability boundary, i.e. the small signal transmission regime, where noise fluctuations will create a new pulse in the cavity. Thus if the transmission window drops below the dotted line, MPI will occur [13, 20]. By concatenating two transmission functions, the effective transmission function can be engineered which allows for significant suppression of the MPI window as a function of input (and output) energy (Fig. 2(b)).

Given the demonstrated suppression of MPI by two transmission functions, it is natural to consider the case of N transmission functions for pushing the MPI instability point out even fur-

#179642 - $15.00 USD Received 12 Nov 2012; revised 13 Feb 2013; accepted 3 Mar 2013; published 8 Mar 2013

ther. The geometrical representation shown in Fig. 2 is a bit simplistic, thus requiring a detailed analysis of a realistic laser cavity. And herein lies one of the significant difficulties of such an analysis: how can one explore the vast parameter space required to achieve realistic results. Indeed, each transmission function (See Fig. 1(b)) has three waveplate settings ($\alpha_{j,1}, \alpha_{j,2}, \alpha_{j,3}$), a polarizer setting ($\alpha_{j,p}$), birefringence adjustment that can be made through polarization ears and gain settings (two parameters). Thus for any single transmission curve, there are seven parameters that nonlinearly effect the resulting transmission function. Optimizing over a single transmission function is already a difficult task. Optimizing over multiple transmission functions is almost intractable. However, we have developed a genetic algorithm that systematically explores viable solutions and optimizes cavity energy and performance. With the very recent advent of electronically controlled waveplates and polarizers [23], it is not difficult to imagine combining the electronic control with the genetic algorithm to achieve significant improvements in mode-locking performance as well optimal cavity design and control.

In what follows, we will consider optimizing over multiple NPR settings in order to demonstrate the proof-of-concept. However, in practice, having so many NPRs can be prohibitively expensive as each NPR incorporates into the cavity three new waveplates, one polarizer, and an additional amplifier. Although 2 NPRs may be somewhat cost effective in doubling cavity energy and power, a more low-cost and feasible alternative to the many NPRs considered here is the incorporation of NOLMs whose periodic transmission function can be similarly be engineered.

3. Governing equation

In order to verify the theoretical predictions of energy enhancement obtained by multiple transmission filters, full simulations of the laser cavity are necessary. The model for describing each fiber section and laser component shown in Fig. 1 can be divided into two parts [12, 24]: (i) the fiber propagation dynamics which includes the interaction of chromatic dispersion, self-phase modulation, birefringence, cavity attenuation/loss, and bandwidth limited gain and saturation, (ii) the discrete effect of the waveplates and polarizers modeled by Jones matrices [12, 24]. The effect of the discrete components is to produce an effective saturable absorption effect on the propagation. These components are often lumped into the governing equations and their sinusoidal transmission approximated through a Taylor expansion [12], this produces the Haus master equation [2]. However, the full sinusoidal transmission can be retained if one is interested, as we are, in producing solutions which are stable in the higher transmission window peaks [12].

The normalized intra-cavity dynamics in j-th fiber section is modeled by coupled nonlinear Schrödinger equations (CNLS) [25, 26]:

$$i\frac{\partial u}{\partial z} + \frac{D_j}{2}\frac{\partial^2 u}{\partial t^2} - K_j u + (|u|^2 + A|v|^2)u + Bv^2u^* = iR_j u \tag{2a}$$

$$i\frac{\partial v}{\partial z} + \frac{D_j}{2}\frac{\partial^2 v}{\partial t^2} - K_j v + (|v|^2 + A|u|^2)u + Bu^2v^* = iR_j v \tag{2b}$$

where u and v represent two orthogonally polarized electric field envelopes in the j-th fiber section of an optical fiber with birefringence K_j. The variable z denotes the propagation distance which is normalized by the length of the first fiber section and t is the retarded time normalized by the full-width at half-maximum of the pulse. The parameter D_j is the averaged group velocity dispersion of the fiber section. It is positive for anormalous dispersion and negative for normal dispersion. In the ANDi laser configuration, which we consider in this paper, D_j is always negative [9]. The nonlinear coupling parameters A (cross-phase modulation) and B (four-wave mixing) are determined by the material of the optical fiber. For axially symmetric

#179642 - $15.00 USD Received 12 Nov 2012; revised 13 Feb 2013; accepted 3 Mar 2013; published 8 Mar 2013

fibers $A+B=1$ and $A=2/3$. The right hand side of the equations, which are dissipative terms, account for the bandwidth limited gain saturation and attenuation, where the operator R_j of the dissipative terms is defined as follows [12]:

$$R_j = \frac{2g_{0,j}}{1+\frac{1}{e_{0,j}}\int_{-\infty}^{\infty}(|u|^2+|v|^2)dt}\left(1+\tau_j\frac{\partial^2}{\partial t^2}\right)-\Gamma_j \tag{3}$$

Here, $g_{0,j}$ and $e_{0,j}$ are the nondimensional pumping strength and the saturating energy of the gain respectively for each fiber section. Parameter τ_j characterizes the bandwidth of the pump, and Γ_j measures the losses (taken to be distributed) caused by the output coupling and the fiber attenuation.

The effect of the waveplates and polarizer is modeled by their corresponding Jones Matrices. The standard Jones matrices of the quarter-waveplate, half-waveplate and polarizer are given, respectively, by:

$$W_{\frac{\lambda}{4}} = \begin{pmatrix} e^{-i\pi/4} & 0 \\ 0 & e^{i\pi/4} \end{pmatrix} \tag{4a}$$

$$W_{\frac{\lambda}{2}} = \begin{pmatrix} -i & 0 \\ 0 & i \end{pmatrix} \tag{4b}$$

$$W_p = \begin{pmatrix} 1 & 0 \\ 0 & 0 \end{pmatrix} \tag{4c}$$

The Jones matrices are valid only when the principle axes of the device is aligned with the fast axis of the fiber. However, this is not generically the case. For an arbitrary orientation given by $\alpha_{j,k}$ ($k=1,2,3,p$), the Jones matrices are modified so that

$$J_k = R(\alpha_{j,k})WR(-\alpha_{j,k}) \tag{5}$$

where W is one of the given Jones matrices and R is the rotation (alignment) matrix:

$$R(\alpha_k) = \begin{pmatrix} \cos(\alpha_{j,k}) & -\sin(\alpha_{j,k}) \\ \sin(\alpha_{j,k}) & \cos(\alpha_{j,k}) \end{pmatrix} \tag{6}$$

This provides a full characterization of the waveplates and polarizers along with their alignment back to the fiber itself.

The CNLS model together with the Jones matrices provides a full description of pulse propagation and mode-locking dynamics in the laser system shown in Fig 1. The full simulation of the multiple filters laser system involves iterations (or round trips in the cavity) of solving the CNLS and then applying the Jones matrices of waveplates and polarizers for each fiber section consecutively in the sequence shown in the experimental configuration. The discrete application of Jones matrices after each cavity round trip acts like a filter that can be tuned to control the mode-locking behavior. Indeed, the waveplate and polarizer settings are critical in engineering the transmission curves $T_n(E)$ for each segment in the laser cavity. The ability to mode-lock pulses is generally closely related to the orientations of the Jones matrices.

4. The genetic algorithm for optimizing laser performance

The addition of NPRs to the laser cavity has already been demonstrated to improve mode-locking performance [20]. But the results presented by Li et al. [20] were limited to two NPRs since no strategy was developed for optimizing the extremely large parameter space generated by the waveplates and polarizers. The current manuscript solves this problem by proposing a

#179642 - $15.00 USD Received 12 Nov 2012; revised 13 Feb 2013; accepted 3 Mar 2013; published 8 Mar 2013

genetic algorithm for searching through the high-dimensional, and highly-nonlinear, parameter space. This allows for a constructive, algorithmic search through parameter space to optimize not only the parameter settings, but to ensure that the laser mode-locks.

In the full cavity model (2)-(6), each additional NPR brings in, at minimum, six additional parameters into the mode-locking dynamics: $\alpha_{j,1}$,$\alpha_{j,2}$,$\alpha_{j,3}$,$\alpha_{j,p}$,$e_{0,j}$ and $g_{0,j}$. For what follows, we will assume that the birefringence K is constant. This parameter can also be easily brought into the optimization procedure. As a consequence, each new NPR (and existing NPR as well) needs to be tuned so that the model produces mode-locking. By adjusting the value of existing NPR parameters along with the new introduced NPR parameters, the goal is produce a mode-locked state whose optimal output energy exceeds its previous optimal value. Due to the fact that the full cavity model is highly nonlinear, i.e. it is governed by nonlinear partial differential equation with discrete components, there are few optimization strategies capable of addressing the best performance as a function of its NPR parameters. Simply sweeping through parameter space ultimately leads to an intractable problem as each NPR gives six degrees of freedom in a sweep search. Thus brute force methods will fail, especially as the number of NPR components are added to the cavity. One of the few algorithms available capable of optimizing such a system is the genetic algorithm, which belongs to the family of evolutionary algorithms. Although there are no guarantees about its ability to convergence we choose the genetic algorithm because the genetic algorithm is one of the few effective methods for dealing with complicated optimization problems where nonlinear or discontinuous constraints are imposed and traditional method no longer hold.

The genetic algorithm is a searching routine that mirrors the process of natural evolution and genetic mutations. That is, it evolves a population of feasible solutions towards potentially better solutions. In particular, given a set of feasible trial solutions (one pulse per round trip mode-locked states), an objective function (the energy) is evaluated. In the next step, solutions that give the minimum (maximum energy) values of the objective function are kept and mutated (perturbed) in order to potentially achieve a better minimization. This process is repeated through a number of iterations, or generations, with the hope that better and better solutions are generated.

To be more precise about the algorithm, consider the parameter optimization problem for the full cavity model. Since we are looking for the parameters that generate one-pulse mode-locked solutions with the maximum pulse energy, the objective function is constructed as follows

$$minimize\,[-E(\mathbf{x})N(\mathbf{x})] \tag{7}$$

where vector $\mathbf{x}$ contains all the parameters of the full cavity model, i.e. the waveplate and polarizer settings, for example, and

$$E(x) = \int_{-\infty}^{\infty} |u|^2 + |v|^2 dt \tag{8}$$

, is the mode-locked pulse energy ($E > 0$) with the indicator function

$$N(\mathbf{x}) = \begin{cases} 1 & \text{For stationary single pulse solution} \\ 0 & \text{Else} \end{cases} \tag{9}$$

Recall that u and v are solutions to the full cavity model described in Section 3. Different techniques can be applied to recognize whether the solution generated represents a single mode-locked pulse per round trip, thereby determining the value of the indicator function $N(\mathbf{x})$. Thus the indicator function throws out all solutions that are not mode-locked or represent two or more pulses per round trip.

#179642 - $15.00 USD Received 12 Nov 2012; revised 13 Feb 2013; accepted 3 Mar 2013; published 8 Mar 2013

Suppose that m initial guesses are given for vector $\mathbf{x}$ and denote that the the i-th initial guess as $\mathbf{x}_i$ where $i = 1, 2, ..., m$. In next step (generation), m solutions of the full cavity model and the corresponding energies are computed. The simulation of the laser dynamics starts from initial white noise and it is simulated over a sufficiently long time so that mode-locking, if it is in a favorable parameter regime, occurs. The energies of the mode-locked solutions (non mode-locked states are discarded) are compared with each other after each generation and ordered so that the first $p < m$ gives the smallest values of the objective function. Then,

$$\mathbf{x}_i, i = 1, 2, ..., p$$

are kept while

$$\mathbf{x}_i, i = p+1, p+2, ..., m$$

are discarded. As a supplement to the $m-p$ discarded parameter sets, $m-p$ new trial parameter sets ($\mathbf{x}_k$ where $k = m-p, ..., m$ are randomly mutated from the p best objective function values. This process is repeated for a finite number of generations. One can also build a control loop on the algorithm which enables the algorithm to continue runing until the objective function value potentially converges.

Note that in order to implement the genetic algorithm parameter search, we are required to solve for the full cavity evolution (2) along with repeated application of N NPR waveplates and polarizers. Thus there are $6\times N$ parameters that are adjusted during the genetic algorithm search. Moreover, the computational cost is significant given that full laser cavity simulations over hundreds of roundtrips is required in order to determine if the solution has mode-locked to a single pulse per round-trip state. Such a method is extremely computationally cumbersome. Thus to save computation time, a multi-grid genetic algorithm is developed, the idea is to first do a genetic algorithm search on a course grid. If it converges, another round of genetic algorithm search in a smaller range based on the previous result is conducted on a finer (more expensive) grid. This helps in efficiently using the genetic algorithm and exploring the parameter space.

In practice, a real laser cavity has many advantages over the computational model developed here. In particular, mode-locking in a real cavity happens on the order of milliseconds or less. Thus, one can imagine implementing the above genetic algorithm where an evaluation of an entire generation could potentially happen in less than a minute using electronic servo controls as suggested in Ref. [23]. This could lead to a cavity self-tuning for optimal mode-locking in a matter of several minutes or tens of minutes. And once tuned, the genetic algorithm could *control* the system by keeping it close to the ideal, optimized energy state. Given the factor of five enhancement in the energy achieved in mode-locking, this is an attractive option which is feasible in practice. It should also be noted that the proposed algorithm could also be modified to find the *dissipative soliton resonance* curve and enforce the precise balance of physical effects leading to an increase mode-locked pulse energy [21, 22]. Thus the genetic algorithm has broader functionality than that advocated and specified here.

5. Simulation results

To demonstrate the results of the genetic algorithm and associated energy enhancement from using multiple transmission filters, simulations of the governing equations (2)-(6) are performed. The simulations are done using a spectral-based methods where the equation is solved in the Fourier domain for the time (spatial-like variable) and advanced in propagation distance (time-like variable) using an adaptive 4th-order Runge-Kutta stepper. The primary advantage of the technique is the highly advantageous accuracy properties of the spectral representation.

Simulation results for the laser cavity are performed for 1-, 2-, 3-, 4-, 5- and 6-NPR filters, i.e. the genetic algorithm is used to optimize each of these cavity configurations by prescribing the best settings for the waveplates and polarizers in each of the NPR elements. Figure 3

#179642 - $15.00 USD Received 12 Nov 2012; revised 13 Feb 2013; accepted 3 Mar 2013; published 8 Mar 2013

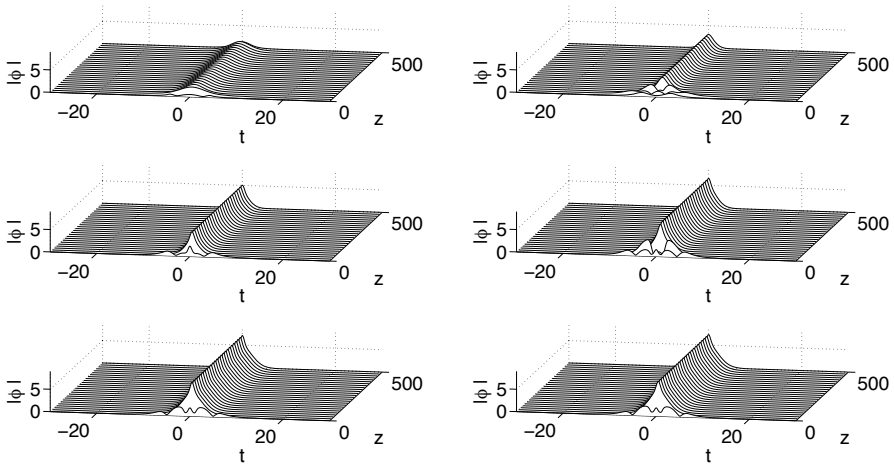

Fig. 3. Optimal mode-locking dynamics achieved for a laser cavity with 1-, 2-, 3-, 4-, 5- and 6-NPR filters (top left to bottom right). A factor of 5 improvement can be made with the inclusion of additional filters.

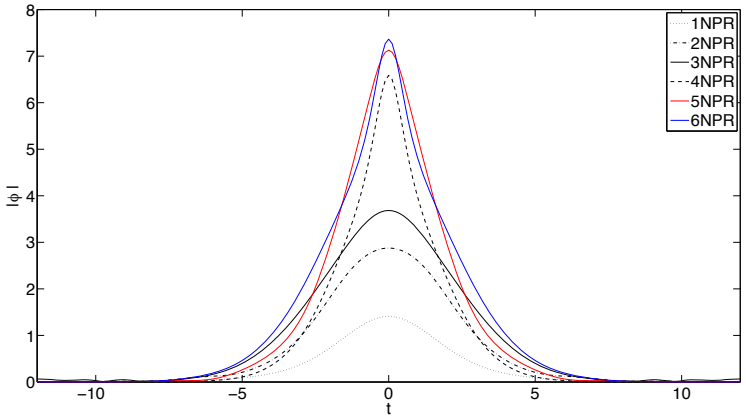

Fig. 4. Optimal mode-locking dynamics achieved for a laser cavity with 1-, 2-, 3-, 4-, 5- and 6-NPR filters (top left to bottom right). A factor of 5 improvement can be made with the inclusion of additional filters.

demonstrate the stable mode-locking dynamics for each of these cases. The initial condition in each case is a white-noise (cold cavity) start. Thus the mode-locked states demonstrated can be achieved in practice. It is clear from the dynamics that mode-locking is quickly achieved and that the more NPRs, the higher the peak power and energy in the mode-locked pulse. The demonstrated mode-locked states are just below the MPI threshold and represent the best performance for each cavity considered. Figure 4 shows a direct comparison of the mode-locked pulse shapes for the cavity with 1-, 2-, 3-, 4-, 5- and 6-NPR filters. Note that the cavity energy

#179642 - $15.00 USD Received 12 Nov 2012; revised 13 Feb 2013; accepted 3 Mar 2013; published 8 Mar 2013

Table 1. Pulse Energy

1NPR	2NPR	3NPR	4NPR	5NPR	6NPR
2.4976	5.5611	6.5144	9.2303	11.2576	11.3226

Table 2. Waveplate and polarizer settings for optimizing 5-NPRs

	$\alpha_{1,j}$	$\alpha_{2,j}$	$\alpha_{3,j}$	$\alpha_{p,j}$	$g_{0,j}$	$e_{0,j}$
j=1	0.0000^0	72.0000^0	38.4740^0	79.2824^0	1.9502	1368.2425
j=2	0.0000^0	72.0000^0	32.3239^0	72.0000	1.8339	1.0000
j=3	0.0000^0	85.3534^0	41.0947^0	72.0000	1.5497	0.6477
j=4	0.0000^0	81.2847^0	38.7435^0	85.8394	1.0000	2.0000
j=5	0.0000^0	90.8970^0	37.4666^0	72.0000	1.9619	0.3786

and peak power increases as the number of NPR filters are added. However, it is found through computation that beyond 5 NPR filters, there appears to be little or no increase in the optimal pulse energy and peak power. Thus using 5-NPRs seems to maximize the laser performance at about 5 times the single NPR cavity energy. Table 1 gives the (normalized) energy achieved for the mode-locked states shown in Figs. 3 and 4. In our simulation studies, it was first necessary to find a set of parameters that enabled stable mode locking. This was then used as the starting point for the optimization performed by the genetic algorithm. As an illustration of the optimization routine, Table 2 shows the various polarizer settings required for the 5-NPR filter.

6. Conclusions

Although the MPI effect is ubiquitous in fiber laser cavities, our theoretical and computational studies suggest that it can be circumvented and suppressed by engineering the transmission function appropriately. As a result, significant pulse energy enhancements are possible. Numerical simulations which include component by component modeling of the fiber laser cavity using the standard coupled nonlinear Schrödinger equation model along with Jones matrices for the waveplates and polarizers shows that the addition of additional NPR filters are capable of significantly enhancing mode-locking performance. In our numerical simulations, a two-fold energy increase is achieved under the 2-NPR configuration, while a factor of 2.6, 3.7 and 4.5 increase is achieved for 3-NPR, 4-NPR and 5-NPR configurations respectively. The addition of NPRs for mitigating MPI and increasing cavity energies is critical in the effort to close the order of magnitude gap in energy performance between fiber lasers and their solid-state counterparts.

To implement the multiple NPR scenario in practice, a new strategy is developed to optimize the cavity performance in the vast parameter space represented by the multiple NPRs. In particular, the key difficulty present in engineering an appropriate transmission function for each NPR concerns the selection of the parameters for the extra NPRs (waveplates, polarizers, gain, etc). As a results, we developed a multigrid genetic algorithm with a built-in pulse recognition routine as the parameter optimization tool. It is a viable and efficient method for searching the high-dimensional parameter space for physically realizable parameter settings which allow for higher single-pulse energies. Indeed, this algorithm can be adopted and modified as a control algorithm for implementation in a physically realizable fiber laser where electronic control can be established over the various parameters [23]. This control algorithm would enable one to control the pulse energy, peak power, bandwidth etc. in the laser cavity dynamically even under the influence of perturbations (changes in temperature, birefringence, position of polarizers).

As a consequence of this work, a multi-NPR configuration with a multi-grid genetic algo-

#179642 - $15.00 USD Received 12 Nov 2012; revised 13 Feb 2013; accepted 3 Mar 2013; published 8 Mar 2013

rithm control loop is established as a highly desirable design tool for engineering high-energy laser cavities. It can allow one to build a more stable, reliable, self-adjusting, cost-efficient and most importantly, high-energy fiber laser system that can compete directly with their solid state counterparts. And as a final note, one can imagine switching the NPR devices considered here, i.e. sets of waveplates and polarizer, with a much cheaper all-fiber based NOLM or NALM device. Indeed, given the prohibitively high cost of inserting additional NPRs (3 waveplates, one polarizer, and an additional amplifier), low-cost alternatives are critical to assessing the success of the multi-transmission curve engineering. Initial indications suggest that the additional amplifiers can be removed from the cavity while retaining close to the same performance gains observed here. Moreover, by replacing the three waveplates and polarizer with a NOLM, for instance, further reduction in cost can be achieved without sacrificing the projected performance gains. What is so compelling about the genetic algorithm implementation is that it simply does not care about the specific details of implementation. Rather, it measures the performance directly of the laser cavity and tunes the parameters it is allowed in order to achieve optimal performance. This is especially important when using a NOLM in the cavity as many of the leading theories for NOLMs are arrived at using simplifications that do not hold in practice, thus rendering the theoretical portion suspect in the optimization process. The genetic algorithm would make direct use of experiment versus theory in tailoring the NOLM settings for enhanced energy production. Such considerations will be made in future work.

Acknowledgments

J. N. Kutz acknowledges support from the National Science Foundation (NSF) (DMS-1007621) and the U.S. Air Force Office of Scientific Research (AFOSR) (FA9550-09-0174).

#179642 - $15.00 USD Received 12 Nov 2012; revised 13 Feb 2013; accepted 3 Mar 2013; published 8 Mar 2013